THERMOPHYSICAL ANALYSIS OF THE PROCESSES OF SOLIDIFICATION, COOLING, AND HEATING OF INGOTS (CASTINGS)

V. I. Timoshpol'skii, É. A. Gurvich, I. A. Trusova, and N. L. Mandel'

UDC 621.783.224.1

The article suggests a mathematical model of the joint heat-engineering process of heating and cooling incompletely solidified ingots.

Problems of heat transfer in bodies with movable phase boundaries (in our case upon solidification of ingots or castings) belong to the most complex problems of the theory of heat conduction. In solving them it is necessary, together with the temperature function, to find a function characterizing the position of the boundaries of phase transitions. This pair of functions is determined by a system of nonlinear differential equations. As a rule, it is not possible to obtain an accurate solution of problems of heat conduction in case of phase transformations because these problems are nonlinear.

In the Soviet and non-Soviet literature there are extensive descriptions of different numerical methods for solving a similar class of problems [1-3, etc.], and the choice of certain calculation and difference schemata is substantiated.

The present article examines the thermal state of a plate ingot in the joint process of its preparation for plastic deformation by a technological procedure as used on the scale of metallurgical production which includes shaping and cooling of the ingot in the ingot mold, cooling in air, and subsequent heating in some appropriate plant.

Complex study of this process is of particular importance for optimizing the heating regime of ingots after hot charging and with an incompletely solidified core; there it is indispensable to know the temperature distribution in the section of the ingot at the instant when it is placed in the heating device.

Let us examine a complex problem, symmetrical about the Oy axis (Fig. 1), of the cooling and heating of a flat (plate) metallurgical ingot obtained by ingot mold casting. Such an arrangement is justified in solving problems for the zone of an industrial ingot situated between one-third and one-half of the height measured from the top of the ingot mold where there is practically no vertical temperature gradient [4].

At all technological stages the temperature field in the ingot is described by the differential equation of nonsteady heat conduction

$$C_i(T)\rho_i(T)\frac{\partial T_i(x,\tau)}{\partial\tau}=\frac{\partial}{\partial x}\left[\lambda_i(T)\frac{\partial T_i(x,\tau)}{\partial x}\right], \tag{1}$$

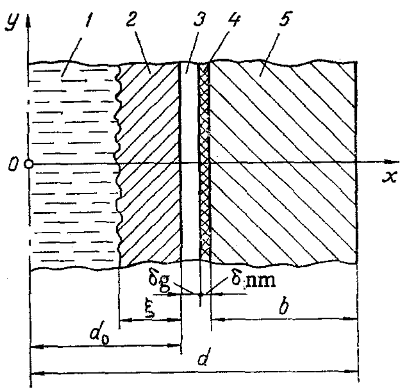

Fig. 1. Advance of the crystallization front in the biphase zone of an ingot (casting): 1) liquid metal; 2) solidifying skin; 3) gas gap; 4) nonmetallic layer on the inner surface of the liquid ingot mold; 5) ingot mold.

Belorussian Polytechnic Institute, Minsk. Translated from Inzhenerno-Fizicheskii Zhurnal, Vol. 54, No. 4, pp. 648-655, April, 1988. Original article submitted December 8, 1986.

 0022-0841/88/5404-0452$12.50

where i = 1, 2. The subscript i denotes values relating to the ingot in the range $0 \le x \le d_0$, the subscript i = 2, those relating to the ingot mold in the range $d_0 \le x \le d$.

Proceeding from the hypothesis that a small section of the ingot mold is filled with liquid melt, we write the initial conditions:

$$T(x;\ 0) = \begin{cases} T_{1,0} & \text{for the ingot,} \\ T_{2,0} & \text{for the mold.} \end{cases} \tag{2}$$

Let us formulate the boundary conditions. On the axis of symmetry (x = 0) the following equation applies:

$$-\lambda_1 \frac{\partial T_1}{\partial x} = 0. \tag{3}$$

At the period of solidification of the ingot in the mold, the conditions of conjugation of the temperature fields in the plane of contact of the ingot and the mold, with a view to the appearance of a gaseous interlayer and a nonmetallic layer on the inner surface of the mold, are the following [3]:

$$-\lambda_2(T)\frac{\partial T_2}{\partial x} = \frac{(T_1 - T_{\text{nm}})\left(\frac{\lambda_g}{\delta_g} + \alpha_{\text{rc}}\right)\frac{\lambda_{\text{nm}}}{\delta_{\text{nm}}}}{\frac{\lambda_{\text{nm}}}{\delta_{\text{nm}}} + \frac{\lambda_g}{\delta_g} + \alpha_{\text{rc}}} = -\lambda_1(T)\frac{\partial T_1}{\partial x}. \tag{4}$$

When the ingot has been knocked out of the mold and is heated in the furnace, the following boundary condition applies to the surface of the ingot:

$$-\lambda_1(T)\frac{\partial T_1}{\partial x}\bigg|_{x=d_0} = \begin{cases} \alpha_c (T_1 - T_0) + \varepsilon\sigma_0 (T_1^4 - T_0^4) & \text{in air cooling,} \\ \alpha_c^{\text{fur}} (T_{\text{fur}} - T_1) + \varepsilon^*\sigma_0 (T_{\text{fur}}^4 - T_1^4) & \text{in furnace heating} \end{cases} \tag{5}$$

On the free surfaces of the ingot mold, where convective and radiative heat exchange with the medium surrounding the mold takes place, the boundary conditions are written in the form:

$$-\lambda_2(T)\frac{\partial T_2}{\partial x}\bigg|_{x=d} = \alpha_c (T_2 - T_0) + \varepsilon\sigma_0 (T_2^4 - T_0^4). \tag{6}$$

When there is a smooth interface between the liquid and the solid phases in the ingot, the equation of heat balance is used:

$$\left(\lambda_1 \frac{\partial T}{\partial x}\right)_{\text{so}} - \left(\lambda_1 \frac{\partial T}{\partial x}\right)_{l} = \rho_1 L \frac{d\xi}{d\tau}.$$

We note that most industrial alloys crystallize in the temperature interval $[T_{\text{liq}}, T_{\text{sol}}]$. The existence of an interval of crystallization with nonuniform temperature distribution leads to the blurring of the boundary between the solid and liquid phases. In that case we have the so-called biphase zone which consists in the intertwining of dendritic crystals with the melt [2]. The effect of liberation of the latent heat of crystallization can be taken into account by introducing into Eq. (1) the effective specific heat instead of C_i:

$$C_{\text{ef}} = \begin{cases} C_{\text{so}}(T) & \text{for } T_1 < T_{\text{sol}} \\ C(T_{\text{sol}}) - L\frac{d\psi}{dT} & \text{for } T_{\text{sol}} < T_1 < T_{\text{liq}}, \\ C_l & \text{for } T_1 > T_{\text{liq}}. \end{cases}$$

The subscripts l and so indicate the liquid or solid state of the alloy.

The volume ratio of solid phase in unit volume of the biphase zone q is determined from the binary Fe–C diagram by the "lever rule:"

$$q = \frac{C_l - C_0}{C_l - C_{\text{so}}} = q(T).$$

To generalize the solution and for convenience of the computation process we introduce the dimensionless temperature $U_i = (T_i - T_0)/T_0$ and the dimensionless coordinate $y = x/d$. Then $T_i = U_i T_0 + T_0$, $x = yd$. When we differentiate these expressions, we obtain

$$\frac{\partial T_i}{\partial \tau} = T_0 \frac{\partial U_i}{\partial t}; \quad \frac{\partial T_i}{\partial x} = \frac{\partial U_i}{\partial y} \frac{T_0}{d}; \quad \frac{\partial}{\partial x} = \frac{\partial}{\partial y} \frac{1}{d}.$$

Substituting these expressions into Eqs. (1)-(6) we obtain a new system in dimensionless form:

$$d^2 C_i(U_i)\rho_i(U_i)\frac{\partial U_i}{\partial t} = \frac{\partial}{\partial y}\left[\lambda_i(U_i)\frac{\partial U_i}{\partial y}\right] \quad \begin{matrix} \text{for } i=1 & 0 \leqslant y \leqslant \frac{d_0}{d}, \\ \text{for } i=2 & \frac{d_0}{d} \leqslant y \leqslant 1; \end{matrix} \tag{7}$$

$$U_i(y;\ 0) = \begin{cases} U_{1,0} & \text{for} \quad y \in \left[0;\ \frac{d_0}{d}\right], \\ U_{2,0} & \text{for} \quad y \in \left[\frac{d_0}{d};\ 1\right]; \end{cases} \tag{8}$$

$$\frac{\partial U_1}{\partial y} = 0 \quad \text{for} \quad y = 0; \tag{9}$$

$$-\lambda_1(U_1)\frac{\partial U_1}{\partial y} = \frac{d(U_1 - U_2)\left(\frac{\lambda_g}{\delta_g} + \alpha_{rc}\right)\frac{\lambda_{nm}}{\delta_{nm}}}{\frac{\lambda_{nm}}{\delta_{nm}} + \frac{\lambda_g}{\delta_g} + \alpha_{rc}} = -\lambda_2(U_2)\frac{\partial U_2}{\partial y}$$

$$\text{for} \quad y = \frac{d_0}{d}; \tag{10}$$

$$-\lambda_1(U_1)\frac{\partial U_1}{dy} = \begin{cases} dU_1\{\overset{v}{\alpha_c} + \varepsilon\sigma_0 T_0^3(U_1+2)[1+(U_1+1)^2]\} \\ d(U_1 - U_{fur})\{\alpha_c^{fur} + \varepsilon^*\sigma_0 T_0^3(U_1 + U_{fur} + 2)[(U_1+1)^2 + (U_{fur}+1)^2]\} \end{cases}$$

$$\text{for} \quad y = \frac{d_0}{d}; \tag{11}$$

$$-\lambda_2(U_2)\frac{\partial U_2}{\partial y} = dU_2\{\alpha_c + \varepsilon\sigma_0 T_0^3(U_2+2)[1+(U_2+1)^2]\} \quad \text{for} \quad y = \frac{b}{d}. \tag{12}$$

The set of expressions (7)-(12) determines the stated problem whose solution was carried out on a digital computer SM-1600.

The calculation network for the ingot mold and the ingot was formed in the following way. First the segments $[0;\ d_0/d]$ and $[d_0/d;\ 1]$ were divided into n_1 and n_2, respectively, equal parts each of which on its segment determined the step h_1 or h_2. Then $h_1 = d_0/dn_1$; $h_2 = (d - d_0)/dn_2$, and altogether the number of parts is $N = n_1 + n_2$. The nodes of the network on the segment $[0;\ 1]$ have the coordinates $x_{c+1} = x_k + h_k$, where

$$h_k = \begin{cases} h_1 & \text{for} \quad k = \overline{0,\ n_1 - 1}, \\ h_2 & \text{for} \quad k = \overline{n_1,\ N - 1}. \end{cases}$$

We examine the temperature field on the network at fixed instants $t = \tau \ell$.

To improve the approximation of the boundary conditions containing a derivative, we introduce additionally into the examination a fictitious network with coordinate nodes that overlap by half a step each of the calculation domains.

We write the finite difference analog of Eqs. (7)-(12) on the nodes of the network, using a four-point implicit schema [5]:

$$d^2 C_{i,k}^l \rho_{i,k}^l \frac{U_k^{l+1} - U_k^l}{\tau} = \frac{2}{h_k - h_{k-1}}\left(\lambda_{i,k+\frac{1}{2}}^l \frac{U_{k-1}^{l+1} - U_k^{l+1}}{h_c} - \lambda_{i,k-\frac{1}{2}}^l \frac{U_k^{l+1} - U_{k-1}^{l+1}}{h_{k-1}}\right),$$

where

$$k=\overline{1,\ N-1};\quad k\neq n_1;$$

$$h_k=\begin{cases} h_1 & \text{for}\quad k=\overline{1,\ n_1-1},\\ h_2 & \text{for}\quad k=\overline{n_1+1,\ N-1};\end{cases}$$

$$U_k^0=\begin{cases} U_{1,0} & \text{for}\quad k=\overline{1,\ n_1},\\ U_{2,0} & \text{for}\quad k=\overline{n_1+1,\ N};\end{cases}$$

$$U_{-1}=U_0;$$

$$\left.\begin{aligned} -\lambda^l_{1,k-\frac{1}{2}}\frac{U_{\Phi_1}^{l+1}-U_{n_1+1}^{l+1}}{h_1}&=d\left(\frac{U_{\Phi_1}^{l+1}-U_{k-1}^{l+1}}{2}-U_{\text{п}}\right)\left(\frac{\lambda g}{\delta_g}+\alpha_{\text{rc}}\right)\\ -\lambda^l_{2,k+\frac{1}{2}}\frac{U_{k+1}^{l+1}-U_{\Phi_2}^{l+1}}{h_2}&=\frac{\lambda\text{nm}}{\delta_{\text{nm}}}\cdot d\left(U_{\text{nm}}-\frac{U_{k+1}^{l+1}+U_{\Phi_2}^{l+1}}{2}\right)\end{aligned}\right\}\ \text{for}\quad k=n_1,$$

where

$$U_{\text{nm}}=\frac{\dfrac{(U_{k+1}+U_{\Phi_2})\lambda\text{nm}}{2\delta\text{nm}}+\dfrac{(U_{k-1}+U_{\Phi_1})}{2}\left(\dfrac{\lambda\text{nm}}{\delta_g}+\alpha_{\text{rc}}\right)}{\dfrac{\lambda\text{nm}}{\delta_{\text{nm}}}+\left(\dfrac{\lambda g}{\delta_g}+\alpha_{\text{rc}}\right)}\quad\text{for}\quad\delta_g\neq 0,$$

$$U_{\text{nm}}=\frac{U_{\Phi_1}+U_{\Phi_2}}{2}\quad\text{for}\quad\delta_g=0;$$

for $k = n_1$

$$-\lambda^l_{1,n_1-\frac{1}{2}}\frac{U_{n_1}^{l+1}-U_{n_1-1}^{l+1}}{h_1}=d\,\frac{U_{n_1-1}^{l+1}+U_{n_1}^{l+1}}{2}\Bigg\{\alpha_c^{e}+$$

$$+\varepsilon\sigma_0T_0^3\left(\frac{U_{n_1}^{l+1}+U_{n_1-1}^{l+1}}{2}+2\right)\left[1+\left(\frac{U_{n_1}^{l+1}-U_{n_1-1}^{l+1}}{2}-1\right)^2\right]\Bigg\},$$

$$-\lambda^l_{1,n_1-\frac{1}{2}}\frac{U_{n_1}^{l+1}-U_{n_1-1}^{l+1}}{h_1}=d\left(\frac{U_{n_1-1}^{l+1}+U_{n_1}^{l+1}}{2}-U_{n_1}^{l+1}\right)\Bigg\{\alpha_c^{\text{fur}}+$$

$$+\varepsilon^*\sigma_0T_0^3\left[\frac{U_{n_1}^{l+1}+U_{n_1-1}^{l+1}}{2}+U_{\text{fur}}^{l+1}+2\right]\left[\left(\frac{U_{n_1-1}^{l+1}+U_{n_1}^{l+1}}{2}+1\right)^2+(U_{\text{fur}}^{l+1}+1)^2\right]\Bigg\},$$

for $k = N$

$$\lambda^l_{2,N-\frac{1}{2}}\frac{U_N^{l+1}-U_{N-1}^{l+1}}{h_2}=d\,\frac{U_{N-1}^{l+1}+U_N^{l+1}}{2}\Bigg\{\alpha_c+$$

$$+\varepsilon\sigma_0T_0^3\left(\frac{U_N^{l+1}+U_{N-1}^{l+1}}{2}+2\right)\left[1+\left(1+\frac{U_N^{l+1}+U_{N-1}^{l+1}}{2}\right)^2\right]\Bigg\}.$$

The system of the last equations with respect to the temperatures in the nodes of the network is solved by the method of matching [5]:

$$U_k=\gamma_k+\beta_kU_{k+1};$$

$$\gamma_k=\frac{D_k-A_k\gamma_{k-1}}{\beta_k+A_k\beta_{k-1}};\quad \beta_k=\frac{C_k}{B_k+A_k\beta_{k-1}};\qquad k=\overline{1,\ N-1};$$

$$\text{for}\quad k=0\quad \gamma_k=0,\quad \beta_k=1;$$

$$A_k=\frac{\lambda^l_{i,k-\frac{1}{2}}}{h^2_{k-1}};\quad B_k=-\left[\frac{d^2C^l_{i,k}\rho^l_{i,k}}{\tau}+\frac{1}{h_k^2}\left(\lambda^l_{i,k+\frac{1}{2}}+\lambda^l_{i,k-\frac{1}{2}}\right)\right];$$

$$C_k=\frac{\lambda_{i,k+\frac{1}{2}}}{h_k^2};\quad D_k=-\frac{d^2C^l_{i,k}\rho^l_{i,k}U^l_k}{\tau}.$$

The matching coefficients for calculating the temperatures $U_{\Phi 1}$, $U_{\Phi 2}$ are found from the corresponding boundary conditions:

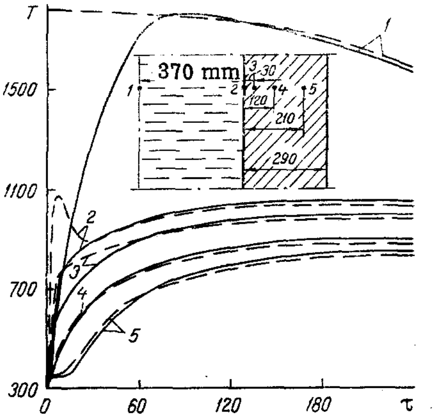

Fig. 2. Comparison of the experimental and theoretical temperature curves in a plate ingot during solidification and cooling in a cast-iron ingot mold; points 1-5 are the places where thermocouples are set; solid curves: experiment [6], dashed curves: calculation on an SM-600 computer. T, K; τ, min.

$$\beta_{U_{\Phi_1}} = \frac{W - X}{Y\beta_{n_1-1} - Z\beta_{n_1-1} - Y - Z};$$

$$\gamma_{U_{\Phi_1}} = \frac{\gamma_{n_1-1}(Z - Y) + U_{n_1+1}(W - X) + 2U_{\text{nm}}(X - Z)}{Y\beta_{n_1-1} - Z\beta_{n_1-1} - Y - Z},$$

$$\gamma_{U_{\Phi_2}} = \frac{2XU_{\text{nm}}}{W + X}; \quad \beta_{U_{\Phi_2}} = \frac{W - X}{W + X}.$$

The temperature of the ingot mold on the boundary with the environment (U_N) at the subsequent time step is found from the expression

$$U_N^{l+1} = \gamma_{N-1}(F - E)/[E(\beta_{N-1} - 1) - F(\beta_{N-1} + 1)].$$

Figure 2 presents the results of the calculation of the change of temperatures at different points of the mold section whose wall thickness is equal to 0.29 m, and at the center of the plate ingot, 0.72 m thick, of rimmed steel. For the sake of comparison the experimental curves of the change of temperature at these same points [6] are given. At the initial period the experimental and theoretical curves do not coincide (especially at the center of the ingot and on the inner surface of the ingot mold). This is due to the great inertia of the heat-sensitive elements that are used for measuring the temperatures at the mentioned points. When the indications of the central thermocouple are out of the inertial period, the curves practically coincide. The calculated time of solidification and cooling of the ingot is 10 min longer than the measured time; this amounts to less than 5%. This circumstance confirms the correctness of the approach to the mathematical modeling of thermal processes in the solidification and cooling of plate ingots chosen by the present authors.

Figure 3 presents the results of a series of calculations of the joint heat engineering process of solidification–cooling–heating of a large plate ingot of steel St3, 0.74 m thick. It follows from the presented theoretical thermograms that when ingots are placed in the furnace before they have completely solidified, it is expedient to heat them practically without holding (τ^1_{nm}), and the rate of the temperature rise at the instant when the heating process ends may attain 200°C/h or more in dependence on the amount of liquid phase. It was also shown that a change of the boundary conditions on the surface of the ingot (in this case cooling in the ingot mold and heating in the furnace) has practically no effect on the rate of crystallization of the ingot (casting). On the basis of experience in production and numerical experiments it was established that in each actual case, when ingots (castings) are left to settle, such an amount of liquid phase should be aimed at where their heating time is minimal. However, when the volume of the liquid core is fairly large, e.g., in blooms, the overall heating time may become longer because of the longer holding time connected with the reduced crystallization rate. The amount of liquid phase in the shaping of ingots (castings) is checked according to the surface temperature on the basis of numerical experiments and production data in each actual case with a view to the marque of steel and the geometric dimensions. When fully crystallized ingots are heated, the heating time (τ^2_{nm} and τ^3_{nm}) is determined by the true heat content of the ingot. In that case it is impossible to avoid the process of holding the metal, and the holding time may be considerably longer than the process of raising the furnace temperature until it reaches the control temperature.

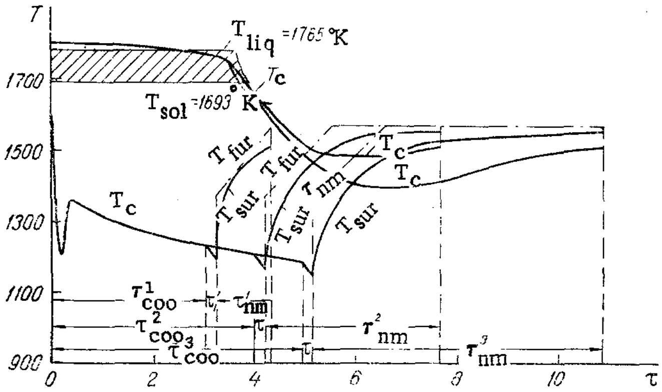

Fig. 3. Thermograms of the joint heat engineering process: τ^1_{coo} = 3 h; τ^2_{coo} = 4 h; τ^3_{coo} = 5 h) cooling time in the ingot mold; τ') cooling in air after "stripping"; τ^1_{nm} = 1 h 5 min) heating with liquid core; τ_{nm} = 3 h 20 min; τ^3_{nm} = 5 h 40 min) heating of completely solidified ingots (castings). τ, h.

Thus, on the basis of our investigations the following conclusions may be reached. A single approach was worked out for the problem of studying the thermal state of large ingots (castings) in the joint technological process of solidification—cooling heating. The interrelation between the regimes of heating and cooling is established by proceeding from the amount of liquid phase and the heat content of hot-charged ingots. Increased volume of the liquid core need not always lead to reduced heating time of ingots (castings); this is also confirmed by the results of numerical experiments concerning the conditions of shaping large plate ingots.

NOTATION

C, ρ, λ) heat capacity, density, and thermal conductivity of the material, respectively; $\alpha_{rc} = \varepsilon_{in}\sigma_0(T_1 + T_{nm})(T_1^2 + T_{nm}^2)$, radiant component of the heat-transfer coefficient from the ingot to the nonmetallic layer on the inner surface of the ingot mold; λ_g and δ_g, thermal conductivity of the gap and its magnitude, respectively; λ_{nm} and δ_{nm}, thermal conductivity of the nonmetallic layer and its magnitude, respectively; ε_{in}, reduced degree of blackness in the system ingot—nonmetallic layer; ε^*, reduced degree of blackness of the surface of the ingot when heated in the furnace; σ_0, radiation factor of a blackbody; α_c, convective component of the heat-transfer coefficient on the surface of the ingot mold; α_c^a, α_c^{fur}, convective component of the heat-transfer coefficient on the surface of the ingot during its cooling in air and during heating in the furnace, respectively; $\xi = \xi(\tau)$, thickness of the solidifying skin in the ingot; L, specific heat of crystallization; T_{sol}, T_{liq}, solidus and liquidus of the alloy, respectively; C_ℓ and C_{so}, concentrations of the component of the alloy depending on the local temperature; T_0, ambient temperature; $U_{\phi 1}$, temperature of the ingot at the node n_1; $U_{\phi 2}$, temperature of the ingot mold at the node n_1; $X = \frac{\lambda_{nm} d}{2\delta_{nm}}$; $Y = \frac{\lambda_{1,n_1-\frac{1}{2}}}{h_1}$; $W = \frac{\lambda_{2,n_1+\frac{1}{2}}}{h^2}$; $Z = \left(\frac{\lambda_g}{\delta_g} + \alpha_{rc}\right)\frac{d}{2}$; $F = \frac{\varphi d}{2}$; $E = \frac{\lambda_{2,N-\frac{1}{2}}}{h_2}$; $\varphi = \alpha_c + \varepsilon\sigma_0 T\left(\frac{U_N^l + U_{N+1}^l}{2} + 2\right)\left[1 + \left(1 + \frac{U_N^l + U_{N-1}^l}{2}\right)^2\right]$.

LITERATURE CITED

1. A. V. Amel'yanchik, I. I. Makarov, T. B. Shirolapova, and E. A. Prokhorova, Inzh.-Fiz. Zh., 24, No. 4, 705-713 (1974).
2. Yu. A. Samoilovich, Shaping of Ingots [in Russian], Moscow (1977).
3. R. I. Es'man, N. P. Zhmakin, and L. I. Shub, Calculations of Casting Processes [in Russian], Minsk (1977).
4. V. D. Maron, K. A. Cherepanov, E. A. Maklov, et al., Izv. Vyssh. Uchebn. Zaved., Chern. Metall., No. 6, 75-79 (1966).
5. A. A. Samarskii, Introduction to Numerical Methods [in Russian], Moscow (1982).

6. É. M. Gol'dfarb, The Heat Engineering of Metallurgical Processes [in Russian], Moscow (1967).

PROPAGATION OF HARMONIC THERMOELASTIC WAVES IN MEDIA WITH THERMAL MEMORY

A. G. Shashkov and S. Yu. Yanovskii

UDC 539.3

We present an analysis of the frequency dependence of phase velocities and damping coefficients of harmonic thermoelastic waves in media with thermal memory.

One of the urgent problems in heat-conduction theory is the investigation of heat-transfer processes taking thermal memory of the material into account [1]. By thermal memory here we mean the influence of the previous history of the thermal state of a body on its current state. Of special interest are the thermoelastic waves in such materials, which have propagation rates and damping coefficients different from the analogous relationships in the classical theory of thermoelasticity. Interest here is also stimulated by experiments on the propagation of thermal impulses at low temperatures [2] and in connection with high intensity thermal effects [3], where deviations from Hooke's Law are observed and where heat propagates at a finite rate in the form of waves of second sound.

A study of planar harmonic thermoelastic waves in the framework of a classical model was made by Chadwick [4]. Engel'brekht studied propagation modes of thermoelastic waves within a model of generalized thermomechanics [5] and within the Green–Lowe model [6].

We consider a one-dimensional mathematical model of linearized intercouple thermoelasticity for isotropic media, taking thermal memory into account [7]:

$$c_v\ddot{\vartheta}(z,\ t)+\tilde{\beta}(0)\dot{\vartheta}(z,\ t)+\int\limits_0^\infty\tilde{\beta}'(s)\dot{\vartheta}(z,\ t-s)\,ds=\tilde{\alpha}(0)\vartheta''(z,\ t)+\int\limits_0^\infty\tilde{\alpha}'(s)\vartheta''(z,\ t-s)\,ds+\varkappa_1\dot{u}'(z,\ t),$$
$$(2\varkappa_3+\varkappa_4)\,u''(z,\ t)-\rho\ddot{u}(z,\ t)=\varkappa_2\vartheta'(z,\ t)+\int\limits_0^\infty\tilde{\gamma}(s)\,\vartheta'(z,\ t-s)\,ds, \tag{1}$$

where a prime indicates differentiation with respect to the coordinate z; differentiation with respect to the time is indicated by an overdot.

We seek a solution of system (1) in the form of planar waves:

$$u=u_0\exp\left[i\left(\eta z-\omega t\right)\right],$$
$$\vartheta=\vartheta_0\exp\left[i\left(\eta z-\omega t\right)\right]. \tag{2}$$

Substituting relations (2) into Eqs. (1), we obtain the following characteristic equation:

$$(c_0^2\eta^2-\omega^2)\left\{c_v\omega^2+i\omega\left[\tilde{\beta}(0)+\tilde{\beta}'_F(\omega)\right]-\eta^2\left[\tilde{\alpha}(0)+\tilde{\alpha}'_F(\omega)\right]\right\}+\eta^2\omega^2\varkappa_1\left[\varkappa_2+\tilde{\gamma}_F(\omega)\right]=0, \tag{3}$$

where $f_F(\omega)$ denotes the Fourier transform of the relaxation function:

$$f_F(\omega)=\int\limits_0^\infty f(s)\exp(i\omega s)\,ds;\quad f=\{\tilde{\alpha}'(s),\ \tilde{\beta}'(s),\ \tilde{\gamma}(s)\}.$$

We write the characteristic equation (3) in dimensionless form:

Institute of Applied Physics, Academy of Sciences of the Belorussian SSR, Minsk. Translated from Inzhenerno-Fizicheskii Zhurnal, Vol. 54, No. 4, pp. 655-662, April, 1988. Original article submitted January 5, 1987.

 0022-0841/88/5404-0458$12.50